Eur Radiol (2016) 26:1775–1782
DOI 10.1007/s00330-015-3994-7

GASTROINTESTINAL

Quantitative assessment of hepatic function: modified look-locker inversion recovery (MOLLI) sequence for T1 mapping on Gd-EOB-DTPA-enhanced liver MR imaging

Jeong Hee Yoon [1] · Jeong Min Lee [1,2] · Munyoung Paek [3] · Joon Koo Han [1,2] · Byung Ihn Choi [1,2]

Received: 16 August 2014 / Revised: 10 June 2015 / Accepted: 1 September 2015 / Published online: 15 September 2015

Abstract

Objectives To determine whether multislice T1 mapping of the liver using a modified look-locker inversion recovery (MOLLI) sequence on gadoxetic acid-enhanced magnetic resonance imaging (MRI) can be used as a quantitative tool to estimate liver function and predict the presence of oesophageal or gastric varices.

Methods Phantoms filled with gadoxetic acid were scanned three times using MOLLI sequence to test repeatability. Patients with chronic liver disease or liver cirrhosis who underwent gadoxetic acid-enhanced liver MRI including MOLLI sequence at 3 T were included (n=343). Pre- and postcontrast T1 relaxation times of the liver (T1liver), changes between pre- and postcontrast T1liver (ΔT1liver), and adjusted postcontrast T1liver (postcontrast T1liver-T1spleen/T1spleen) were compared among Child-Pugh classes. In 62 patients who underwent endoscopy, all T1 parameters and spleen sizes were correlated with varices.

Results Phantom study showed excellent repeatability of MOLLI sequence. As Child-Pugh scores increased, pre- and postcontrast T1liver were significantly prolonged (P<0.001), and ΔT1liver and adjusted postcontrast T1liver decreased (P<0.001). Adjusted postcontrast T1liver and spleen size were independently associated with varices (R^2=0.29, P<0.001).

Conclusions T1 mapping of the liver using MOLLI sequence on gadoxetic acid-enhanced MRI demonstrated potential in quantitatively estimating liver function, and adjusted postcontrast T1liver was significantly associated with varices.

Key Points

- *T1 mapping using MOLLI sequence can be achieved within a breath-hold.*
- *T1liver measured by MOLLI sequence provided excellent short-term repeatability.*
- *Precontrast and postcontrast T1liver were significantly prolonged as Child-Pugh scores increased.*
- *Adjusted postcontrast T1liver and spleen size were independently associated with varices.*

Keywords T1 map · Gadoxetic acid · Magnetic resonance imaging · MOLLI · Liver function estimation

Abbreviations

MOLLI	Modified look-locker inversion recovery
MRI	Magnetic resonance imaging
OATP	Organic anion transporter
T1liver	T1 relaxation time of the liver (ms)
T1spleen	T1 relaxation time of the spleen (ms)
ΔT1liver	Change in T1 relaxation time of the liver before and after Gd-EOB-DTPA administration, divided by the precontrast T1 relaxation time of the liver ([precontrast T1liver-postcontrast T1liver]/precontrast T1liver)
Adjusted postcontrast T1liver	Modulus of the difference between postcontrast T1 relaxation time of the liver, and postcontrast T1 relaxation

✉ Jeong Min Lee
jmsh@snu.ac.kr; jmlshy2000@gmail.com

[1] Department of Radiology, Seoul National University Hospital, Seoul, Korea

[2] Institute of Radiation Medicine, Seoul National University College of Medicine, 101 Daehak-ro, Jongno-gu, Seoul 110-744, Korea

[3] Siemens Healthcare, Seoul, Korea

time of the spleen divided by the postcontrast T1 relaxation time of the spleen ([T1liver-T1spleen]/T1spleen) gadoxetic acid enhanced MR can be used as a quantitative tool for the estimation of liver function and in predicting the presence of oesophageal or gastric varices.

Introduction

Liver function estimation plays an essential role in predicting the prognosis of patients with chronic liver disease (CLD) or liver cirrhosis (LC), both of which ultimately lead to metabolic hepatic failure. Liver function estimation is also an integral part of the therapeutic decision making in patients with hepatocellular carcinoma (HCC) within a background of CLD or LC, and can help physicians make the appropriate treatment decision [1]. Currently, estimation of the hepatic functional reserve is performed using various methods, such as indocyanine green retention at 15 min (ICG R15), hepatobiliary scintigraphy, or hepatic volumetric assessments [2–6]. However, consensus regarding the "reference standard" for the estimation of the hepatic functional reserve has not yet been established.

Gadoxetic acid (Bayer Healthcare, Berlin, Germany), a hepatocyte-specific magnetic resonance (MR) contrast agent, has recently been shown to be useful for the detection and characterization of focal liver lesions (FLLs), particularly HCCs [7–10]. Furthermore, there have been several attempts to use gadoxetic acid for the evaluation of liver function as it is known to be actively taken up by hepatocytes via organic anion transporters (OATPs), similar to ICG [11–14]. Indeed, previous studies have demonstrated that measurement of hepatic parenchymal enhancement on gadoxetic acid-enhanced MRI during the hepatobiliary phase (HBP) may accurately reflect liver function [14–16]. However, direct measurement of hepatic parenchymal signal intensity (SI) is not as simple as it may seem, as SI is not proportional to the concentration of gadoxetic acid, varies greatly depending on the imaging parameters used, and can also be confounded by several technical factors [16]. To the contrary, T1 relaxation times measured by MR relaxometry should be directly correlated, at least theoretically, with the concentration of gadoxetic acid. Therefore, the T1 mapping approach may be more reliable than direct measurement of the SI of the liver especially at 3 T [16, 17]. Among the various T1 mapping methods, a modified look-locker inversion recovery (MOLLI) sequence for T1 mapping has become widely investigated in cardiac imaging [18–20], as it can provide high-resolution T1 maps within a breath-hold. We hypothesized that T1 mapping using MOLLI sequence would also provide good quality T1 mapping for the assessment of liver function and for the prediction of the presence of varices, which is one of the major complications of portal hypertension [21].

Therefore, the purpose of this study is to determine whether multislice T1 mapping of the liver using MOLLI sequence on

Materials and methods

This retrospective study was approved by our institutional review board and the requirement for informed consent was waived. An employee of Siemens (M.P.) provided technical support for optimization of sequence. The authors not associated with Siemens (J.H.Y., J.M.L., J.K.H., and B.I.C.) maintained full control of the data at all times.

Study population

From July 2012 to February 2013, 389 patients underwent gadoxetic acid-enhanced liver MRI including MOLLI sequence. Among them, patients who met one or more of the following inclusion criteria comprised our study population: a) histologically diagnosed hepatitis, b) viral hepatitis based on serology findings (hepatitis B surface antigen positive, hepatitis C antibody positive), c) alcoholic liver disease (ALD) based on patient's history [22, 23], and/or d) characteristic imaging features of LC on cross-sectional images combined with surrogate laboratory findings of cirrhosis [24, 25]. We excluded patients who had a) no history of liver disease and had negative serology findings, b) significant iron depositions in either the liver or spleen parenchyma on the T2* corrected multi-echo chemical shift imaging sequence, c) presence of bile duct obstruction, and d) numerous FLLs which may hinder liver parenchymal evaluation. Finally, 343 patients (M:F=256:87; mean age, 61.1±10.4 years) comprised our study population. Ten patients (M:F=6:4) in whom T1 mapping was acquired at the portal hilum level twice before and after contrast media injection were excluded from our main data analysis, but were included to test the repeatability of T1 mapping using MOLLI sequence. In the remaining 333 patients (M:F=250:83; mean age, 61.1±10.5 years), 11 patients had CLD (M:F=6:5, mean age 56.8±12.2), and 322 patients were classified as having LC: A5 (n=249; M:F=198:62; mean age, 60.6±9.9), A6 (n=44; M:F=29:15; mean age, 63.3±13.9), B7 (n=18; M:F=13:5; mean age, 66.5±6.0), B8 (n=9, M:F=8:1, mean age, 61.9±7.7), and C10 (n=2, M:F=1:1, mean age, 65.5±6.4). Underlying diseases included chronic hepatitis B (n=254); chronic hepatitis C (n=34); ALD (n=21); co-infection of hepatitis B and C (n=2); and non-B-non-C cirrhosis (n=22).

In order to determine whether T1 relaxation times of the liver can predict the presence of varices, we searched for patients who had undergone endoscopy within 3 months of the MR examination. A total of 62 patients (CLD [n=2], LC [n=60]; M:F=48:14; mean age, 60.0±11.1 years) had available

endoscopy results (mean interval between the two exams, 7± 48 days, 95 % CI: 5.0 – 19.4 days). Among them, 26 patients were confirmed to show no signs of varices, while the remaining 36 patients were diagnosed with oesophageal or gastric varices: grade 1 (n=16); grade 2 (n=9); oesophageal varices ligation for bleeding (n=8); and portal hypertensive gastropathy (n=3).

MR imaging acquisition

MR images were obtained at a 3 T unit (Magnetom Verio, Siemens Healthcare, Erlangen, Germany) using a 32-channel torso phased-array coil. Baseline MR sequences included the breath-hold (BH) T2-weighted half Fourier single-shot turbo spin-echo (TSE) sequence, respiratory-triggered T2-weighted TSE, BH T1-weighted 3D spoiled gradient-recalled-echo sequence (GRE), BH T2*-corrected triple-echo spoiled GRE sequence, and diffusion weighted images. After injection of gadoxetic acid (0.025 mmol/kg) at a rate of 1.5 mL/s followed by a 30-mL saline flush, dynamic T1-weighted images were obtained including the arterial, portal venous, and equilibrium phases as well as a 20 min delayed HBP.

MOLLI sequence For T1 mapping, two-dimensional (2D) T1 maps using MOLLI sequence were obtained twice, once before and once 10 min after administration of gadoxetic acid [18]. Three axial slices were obtained at the levels of the intrahepatic inferior vena cava confluence, portal hilum, and gallbladder fossa. MOLLI sequence consisted of three inversion recovery prepared look-locker pulses performed consecutively within a breath-hold [26]. Imaging parameters were as follows: TR/TE=2.5/1.06 ms; flip angle, 35°; number of excitations, 1.0; field of view (FOV), 340x273 mm; matrix, 192x124; acceleration factor, 2; nonselective inversion pulse; steady-state free precession single-shot readout sequence; fixed time interval TR, 700 ms; minimum inversion time (TI), 100 ms; slice thickness, 8 mm; number of inversions, 3; number of acquisitions after an inversion pulse, 3, 3, 5; number of recoveries after each inversion pulse, 4, 4, 0; and TI increment between inversions, 80 ms. Fully automated non-rigid motion correction was applied to register individual images. Thereafter, inline fitting was performed using a mono-exponential, three-parameter fit, and T1 maps were automatically calculated using work-in-progress software provided by the vendor (Siemens Healthcare, Erlangen, Germany).

Phantom measurements for evaluation of repeatability

To confirm the inter-examination repeatability of T1 values obtained using MOLLI sequence on gadoxetic acid-enhanced MRI, and to estimate T1 relaxation time changes according to gadoxetic acid concentrations, six cylindrical tubes (3x3x6 cm) filled with six different concentrations of gadoxetic acid (0.8, 1, 1.4, 1.6, 2.25, and 3 mmol/L) were scanned three times using MOLLI sequence with an interval of 4 days. Room temperature in the MR unit was kept constant at 20 – 21 °C. Imaging parameters were identical to the MR protocol used in patients, except the following items: TR/TE= 3.6/1.48 ms; FOV, 150x150 mm; matrix, 192x192.

Evaluation of the repeatability of T1 relaxation times using MOLLI sequence

Prior to implementation of the T1 mapping sequence using MOLLI, within-subject repeatability of T1 measurements using MOLLI sequence was tested in ten patients (M:F=6:4; mean age, 61.7±7.4 years). Each pre- and postcontrast T1 mapping was performed twice, with an interval of 2 min. Imaging parameters were the same as the protocol described above.

Data analysis

Measurements of T1 relaxation times were made by drawing regions of interest (ROIs) on the T1 maps. In phantoms, one attending radiologist (J.H.Y. with 8 years of clinical experience) measured T1 values by drawing approximately 300 mm^2 sized circular ROIs in the centre of the cylinders on axial T1 maps. For measurement of T1 values in the study patients, one radiologist (J.H.Y.) who was blinded to the Child-Pugh (CP) scores and endoscopy findings, drew free-hand ROIs (mean area, 44.8±22.6 cm^2 in the liver, 6.8± 4.7 cm^2 in the spleen) on each slice of the T1 maps (Fig. 1). ROIs were placed on precontrast T1 maps and then copied and pasted to the postcontrast T1 maps. FLLs and major branches of the hepatic vessels were carefully avoided. Mean values of the ROIs were considered the representative T1 relaxation times of the liver and spleen (T1liver, T1spleen, respectively).

After measurement of T1 relaxation times, two additional parameters (ΔT1liver, adjusted T1liver) were obtained. Changes in T1liver between pre- and postcontrast T1 maps (ΔT1liver) were calculated as follows: ΔT1liver=(precontrast T1liver-postcontrast T1liver)/precontrast T1liver. ΔT1liver was aimed to capture the change in relaxation times owing solely to functioning hepatocytes containing gadoxetic acid [27]. Adjusted postcontrast T1liver was calculated as follows: adjusted postcontrast T1liver=(postcontrast T1liver-postcontrast T1spleen)/postcontrast T1spleen. Adjusted postcontrast T1liver was intended to exclude the enhancement effect of extracellular contrast media from hepatic enhancement on the HBP [13].

In addition, the longest diameter of the spleen was measured on axial post-contrast T1WI by one radiologist (J.H.Y.) in all patients [28].

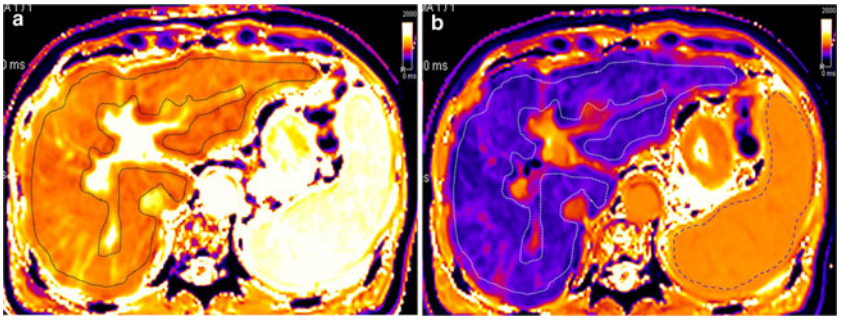

Fig. 1 Precontrast (**a**) and postcontrast (**b**) T1 maps in a 72-year-old man with Child-Pugh score B7. The free-hand drawn region of interest of liver and spleen is shown (*dotted closed curves*). Precontrast T1liver, postcontrast T1liver and T1spleen were 1056 ms, 565 ms and 1069 ms, respectively. Given that, ΔT1liver was 0.46 and adjusted postcontrast T1liver was 0.47

Statistical analysis

Test-retest repeatability was analyzed using the within-subject coefficient of variance (CV) in phantoms and in patients who underwent MOLLI twice [29]. In 333 patients, four variables of T1 maps were compared among patients with different CP scores using the Kruskal-Wallis test followed by post-hoc analysis using Bonferroni correction. The Student t-test was used to compare the four T1 variables and spleen size among Child A and B patients, as well as between varices and non-varices groups. Receiver operating characteristic (ROC) curve analysis was performed to compare the diagnostic performances of T1 variables and spleen size for the assessment of varices as well as decompensated cirrhosis. Finally, logistic regression analysis using the stepwise method was performed to assess significant variables related with decompensated cirrhosis (Child B and C) and varices. A *P*-value of less than 0.05 was determined to indicate a statistical significance. All statistical analyses were performed using commercially available software (MedCalc, version 12, MedCalc Software, Mariakerke, Belgium; IBM SPSS Statistics, version 21.0, SPSS Inc., Armonk, NY, USA).

Results

Changes in T1 relaxation times of the phantom according to gadoxetic acid concentrations and the repeatability of T1 maps

The T1 relaxation time was highest with 0.8 mmol of gadoxetic acid (1101 – 1166 ms) and shortened as the concentration of gadoxetic acid increased (823 – 854 ms in 1 mmol; 744 – 777 ms in 1.4 mmol; 681 – 710 ms in 1.6 mmol; 502 – 527 ms in 2.25 mmol; and 401 – 423 ms in 3 mmol). The three measurements of T1 relaxation times showed excellent repeatability in all concentrations of gadoxetic acid (within-subject CV, 2 – 5.5 % in each concentration). In the ten patients who underwent pre- and postcontrast T1 maps twice, both showed excellent agreement in the liver (799±97 and 798±97, within-subject CV 0.3 % [95 % CI: 0.2 – 0.4]; 309±57 and 307±56, within-subject CV, 1.1 % [95 % CI: 0.6 – 1.4]) and the spleen (1291±109 and 1290±106, within-subject CV, 0.4 % [95 % CI: 0.1 – 0.7]; 817±72 and 823±76, within-subject CV, 0.6 % [95 % CI, 0.3 – 0.5]).

T1 relaxation times of the liver on pre- and postcontrast T1 maps

Compared to patients with CP class A, those with CP class B showed significantly prolonged precontrast T1liver (883±90 vs. 972±162 ms, respectively, $P=0.007$) and postcontrast T1liver (507±143 vs. 337±91 ms, respectively, $P<0.001$). Pre- and postcontrast T1liver was lowest in patients with CLD and A5, and increased as CP scores increased (Table 1, Fig. 2a–b). ΔT1liver and adjusted postcontrast T1liver values were the highest in patients with CP scores of A5 and most diminished in patients with CP class B (Table 1, Fig. 2c–d). According to ROC analysis, adjusted postcontrast T1liver (area under the curve [AUC], 0.87; 95 % CI: 0.83 – 0.91), postcontrast T1liver (AUC, 0.86; 95 % CI: 0.81 – 0.89), ΔT1liver (AUC, 0.85; 95 % CI: 0.80-0.89) showed significantly higher diagnostic performance to differentiate decompensated cirrhosis from Child A than precontrast T1liver (AUC, 0.71; 95 % CI: 0.65 – 0.76) ($P=0.007$ – 0.05).

Logistic regression analysis revealed that the adjusted postcontrast T1liver value alone was significantly associated with decompensated cirrhosis ($P<0.001$). Age, sex, three other MR parameters, and spleen size were not independently significant factors.

Prediction of oesophageal and gastric varices using T1 values of the liver

Patients with varices showed significantly prolonged pre- and postcontrast T1liver, compared to patients without varices (Fig. 3, Table 2). ΔT1liver and adjusted postcontrast T1liver were significantly lower in the varices group than in the

Table 1 T1 values of the liver on pre- and postcontrast T1 maps according to Child-Pugh score

	CLD (*n*=11)	A5 (*n*=249)	A6 (*n*=44)	B7 (*n*=18)	B8 (*n*=9)	C10 (*n*=2)
Precontrast T1liver (ms)	863±81	879±86	909±109	943±170	1042±146	872, 961
Postcontrast T1liver (ms)	278±78	326±84	404±100	467±144	571±129	524, 637
ΔT1liver†	0.68±0.09	0.63±0.08	0.56±0.10	0.51±0.09	0.45±0.09	0.34, 0.4
Adjusted postcontrast T1liver ‡	0.70±0.08	0.65±0.10	0.56±0.12	0.48±0.12	0.40±0.12	0.37, 0.39

Note. *T1liver*, T1 relaxation time of the liver. †, (precontrast T1liver –postcontrast T1liver)/ precontrast T1liver; ‡, (postcontrast T1liver – postcontrast T1spleen)/ postcontrast T1spleen. Values are mean±standard deviation

non-varices group (Table 2, $P<0.001$). In addition, the spleen was significantly larger in the varices group compared to the non-varices group ($P=0.02$). Logistic regression analysis revealed that only adjusted postcontrast T1liver and spleen size were independently associated with varices (AUC, 0.81; 95 % CI, 0.7 – 0.9, $R^2=0.29$, $P<0.001$); the Odds ratios for varices were 0.0004 in adjusted postcontrast T1liver (95 % CI: 0 – 0.09) and 1.6 in spleen size (95 % CI: 1.1 – 2.2). ΔTliver, pre- and postcontrast T1liver, age, and sex were not significantly correlated with varices.

Discussion

Our study results showed that all T1 parameters from pre- or postcontrast T1 maps using MOLLI sequence were significantly different between non-cirrhotic or CP class A and CP class B patients. In addition, adjusted postcontrast T1liver obtained 10 min after injection of gadoxetic acid was significantly associated with oesophageal or gastric varices. Furthermore, in our study, T1 mapping using MOLLI sequence showed excellent short term repeatability. Therefore, as T1 mapping of gadoxetic acid-enhanced MR images using

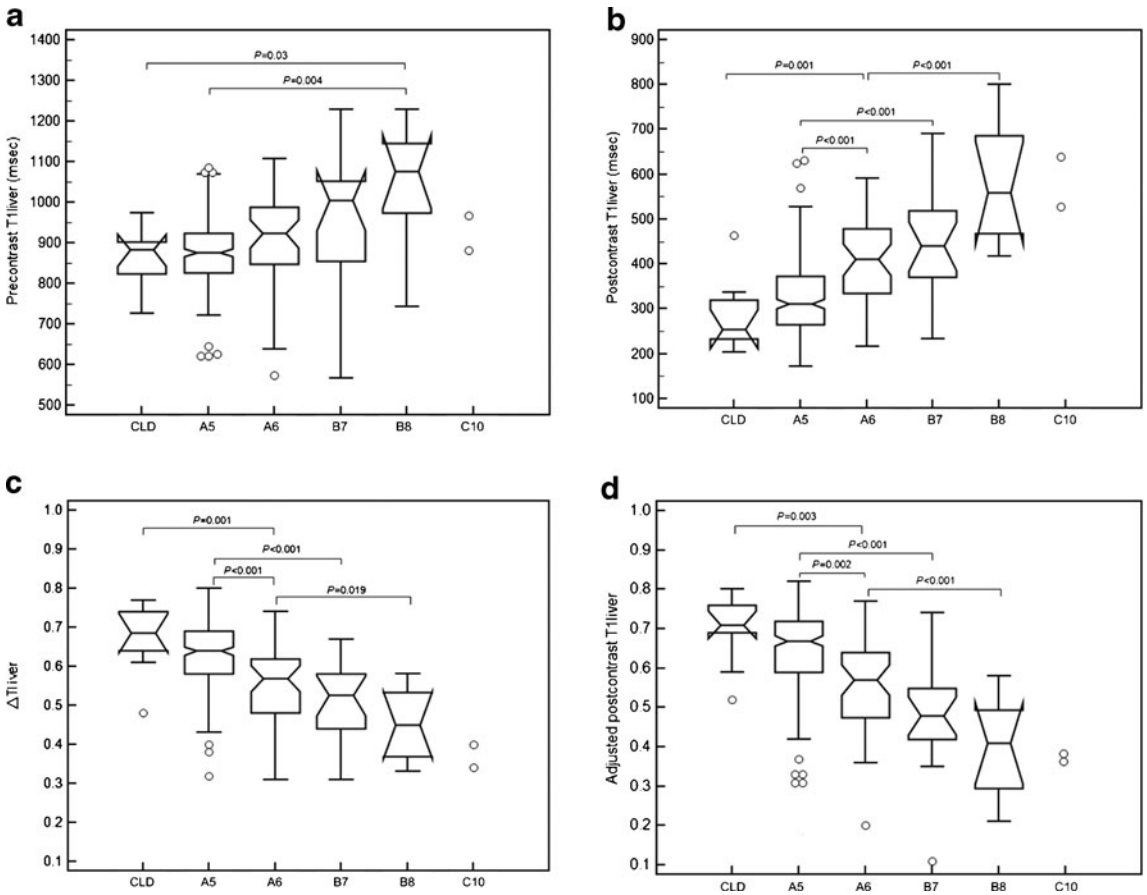

Fig. 2 Calculated T1 parameters and spleen size in patients with different CP scores. **a**. & **b**. Precontrast (**a**) and postcontrast (**b**) T1liver values were significantly higher as Child-Pugh scores increased. **c**. & **d**. ΔT1liver (**c**) and adjusted postcontrast T1liver (**d**) significantly decreased as Child-Pugh score increased

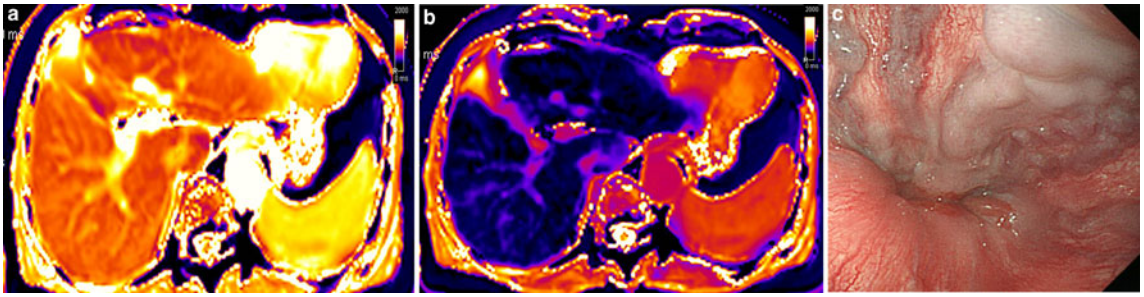

Fig. 3 Pre- and postcontrast T1 maps and endoscopic findings of a patient with a Child-Pugh score of A6. Precontrast T1liver was 993 ms (**a**), postcontrast T1liver was 358 ms and postcontrast T1spleen was 867 ms (**b**). Adjusted postcontrast T1liver was 0.59. Grade I esophageal varices were observed on endoscopy (**c**)

MOLLI sequence can be achieved in a breath-hold and enables accurate stratification of patients with CLD or LC, we believe that T1 measurements using MOLLI sequence has demonstrated potential as a practical method of quantitatively estimating liver function.

In our study, parameters on postcontrast T1 maps showed better capability in differentiating CP class, compared to precontrast T1liver (AUC: 0.85 – 0.87 vs. 0.71, P=0.007 – 0.05). The superior ability of the three parameters of postcontrast T1 maps in grading liver functions in CLD and LC patients can be explained by the pharmacokinetic characteristics of gadoxetic acid. Gadoxetic acid is taken up by hepatocytes via OATPs and excreted into bile via multidrug-resistant protein2 (MRP2) [14]. Studies have shown that the uptake of gadoxetic acid can dwindle as the function of hepatocytes decreases [30] and that this can attribute to the decline in OATP expression and overexpression of MRP2 in diseased livers [15], consequently causing a decline of the T1 shortening effect of gadoxetic acid. Therefore, prolonged postcontrast T1liver, decreased ΔT1liver and adjusted postcontrast T1liver in patients with diminished liver function indicates that a smaller amount of intracellular contrast media remains, which may be the result of reduced hepatic OATP expression in patients with decreased liver function. These results are in line with the results of previous studies [17, 31].

Among the variables of postcontrast T1 maps, adjusted postcontrast T1liver was the only significantly associated factor with varices and decompensated cirrhosis. Adjusted postcontrast T1liver represents T1 shortening via intracellular contrast agents after exclusion of enhancement by contrast media in extracellular space [13, 32], and this may directly show the T1 shortening effect by gadoxetic acid in hepatocytes. To the contrary, postcontrast T1liver and ΔT1liver include all changes in both intracellular and extracellular space after contrast media administration, which may effectively cancel each other out: decreased T1 shortening by decreased uptake of intracellular contrast media and increased T1 shortening by widened extracellular contrast media retention in advanced cirrhosis. This may explain the superior capability of adjusted postcontrast T1liver.

In this study, we also revealed that adjusted postcontrast T1liver and spleen size were independently associated with varices, which is a good marker for portal hypertension. Furthermore, adjusted postcontrast T1liver was able to differentiate Child A5 patients from Child A6, which may have the potential to detect early signs of decompensating cirrhosis.

Table 2 Comparison of T1 map parameters and patient characteristics between the varices and non-varices groups

	Varices group (n=36)	Non-varices group (n=26)	P-value
Sex (M:F)	28:8	20:6	0.85
Age (years)	60±12	60±11	0.80
CP class A:B:C	24:11:1	23:3:0	0.02
Albumin (mg/dL)	3.5±0.5	4.1±0.4	<0.001
Total bilirubin (mg/dL)	2.4±4.7	1.1±0.8	0.18
PT INR (INR)	1.19±0.23	1.06±0.10	0.007
Precontrast T1liver (ms)	951±114	874±105	0.01
Postcontrast T1liver (ms)	462±148	338±91	0.001
▵T1liver †	0.52±0.12	0.62±0.10	0.005
Adjusted postcontrast T1liver ‡	0.50±0.15	0.64±0.11	<0.001
Spleen size (cm)	11.7±1.6	10.8±2.1	0.02

Note. *CP class*, Child-Pugh class; †, (precontrast T1liver –postcontrast T1liver)/precontrast T1liver; ‡, (postcontrast T1liver – postcontrast T1spleen)/postcontrast T1spleen. Values are mean±standard deviation. A P-value less than 0.05 indicates a statistically significant difference between the two groups

Although further validation is warranted by combining and comparing currently available diagnostic tools, we believe that T1 maps using MOLLI sequence has several advantages in detecting portal hypertension in terms of its non-invasive nature, its lack of requirement for anaesthesia, and that it can be achieved in a single breath-hold during liver MRI, compared to hepatic vein catheterization and endoscopy [33, 34].

Until now, various approaches have been used for the assessment of hepatic function using gadoxetic acid-enhanced liver MRI, including measurements of biliary enhancement [16], direct liver SI measurements [35], MR relaxometry [17, 36], or dynamic contrast-enhanced MRI [11]. From a technical aspect, T1 maps obtained using MOLLI sequence may be more robust than simple SI measurements on the HBP [35], as T1 maps are less affected by MR parameters at the same magnetic field strength [37] than SI measurements. Among the T1 mapping techniques, MOLLI has several advantages as it is timely efficient compared to conventional techniques [17], which only samples one point for each inversion pulse. In addition, MOLLI is less sensitive to B1 heterogeneity and less prone to error compared to the variable flip angle method [38, 39]. Another advantage of T1 mapping using MOLLI sequence is its feasibility in clinical practice. Dynamic measurement of parenchymal enhancement may be theoretically more accurate than static measurements, but it is not clinically acceptable owing to its long examination times of up to 90 min [11, 40], although recent study reported the results obtained from standard clinical protocols [41, 42]. In our study, acquisition of T1 mapping using MOLLI sequence required only one breath-hold, and postcontrast T1 maps were able to be obtained 10 min after contrast media injection without prolonging the scan time, and with satisfying differentiating performance in assessing liver function. Therefore, we believe that this technique can be included as a part of routine liver MRI, when needed.

This study has several limitations. First, as this study was of retrospective design, there may have been unavoidable selection bias. Second, a relatively small number of CP class B and C patients were included, since only a limited number of patients with decompensated cirrhosis undergo liver MRI due to supportive management guidelines in the clinical setting. Third, we did not compare T1 relaxation times of the liver with other quantitative liver function tests such as ICG R15 or LiMAX [43, 44]. Fourth, MOLLI sequence is a 2D sequence and, as such, does not cover the whole liver. However, we believe that averaging the T1 values measured from the three slices could represent the T1 values of the liver. In addition, obtaining an additional sequence in addition to the routine sequence may be cumbersome in clinical practice, whereas T1 mapping using MOLLI can be achieved in single breath-hold and would not significantly hamper the clinical workflow. Last, the diagnosis of cirrhosis was not established histologically.

In conclusion, T1 mapping of the liver using MOLLI sequence demonstrated potential in quantitatively estimating liver function by enabling stratification of patients with variable CP scores. In addition, T1 relaxation time measurements of the liver after gadoxetic acid administration may be used to predict the presence of oesophageal or gastric varices.

Acknowledgments We thank Chris Woo (B.A., USA) for his editorial assistance. The scientific guarantor of this publication is professor Jeong Min Lee. Authors of this manuscript declare relationships with the following companies: J.M.L., author received nonfinancial technical support from Siemens Healthcare; M.P, an employee of Siemens Healthcare. The authors state that this research was supported by Basic Science Research Program through the National Research Foundation of Korea (NRF) funded by the Ministry of Education (2013R1A1A2A10066037). No complex statistical methods were necessary for this paper. Institutional Review Board approval was obtained. Written informed consent was waived by the Institutional Review Board. Methodology: retrospective, case-control study, performed at one institution.

References

1. Bruix J, Sherman M (2011) Management of hepatocellular carcinoma: an update. Hepatology 53:1020–1022
2. Kwon A, Ha-Kawa SK, Uetsuji S, Inoue T, Matsui Y, Kamiyama Y (1997) Preoperative determination of the surgical procedure for hepatectomy using technetium-99m-galactosyl human serum albumin (99mTc-GSA) liver scintigraphy. Hepatology 25:426–429
3. Vauthey J-N, Chaoui A, Do K-A et al (2000) Standardized measurement of the future liver remnant prior to extended liver resection: methodology and clinical associations. Surgery 127:512–519
4. Kokudo N, Vera DR, Tada K et al (2002) Predictors of successful hepatic resection: prognostic usefulness of hepatic asialoglycoprotein receptor analysis. World J Surg 26:1342–1347
5. Dinant S, de Graaf W, Verwer BJ et al (2007) Risk assessment of posthepatectomy liver failure using hepatobiliary scintigraphy and CT volumetry. J Nucl Med 48:685–692
6. de Graaf W, van Lienden KP, van Gulik TM, Bennink RJ (2010) 99mTc-mebrofenin hepatobiliary scintigraphy with SPECT for the assessment of hepatic function and liver functional volume before partial hepatectomy. J Nucl Med 51:229–236
7. Kudo M (2010) Will Gd-EOB-MRI change the diagnostic algorithm in hepatocellular carcinoma? Oncology 78(Suppl 1):87–93
8. Inoue T, Kudo M, Komuta M et al (2012) Assessment of Gd-EOB-DTPA-enhanced MRI for HCC and dysplastic nodules and comparison of detection sensitivity versus MDCT. J Gastroenterol 47:1036–1047
9. Granito A, Galassi M, Piscaglia F et al (2013) Impact of gadoxetic acid (Gd-EOB-DTPA)-enhanced magnetic resonance on the non-invasive diagnosis of small hepatocellular carcinoma: a prospective study. Aliment Pharmacol Ther 37:355–363
10. Ahn SS, Kim MJ, Lim JS, Hong HS, Chung YE, Choi JY (2010) Added value of gadoxetic acid-enhanced hepatobiliary phase MR imaging in the diagnosis of hepatocellular carcinoma. Radiology 255:459–466
11. Nilsson H, Blomqvist L, Douglas L et al (2013) Gd-EOB-DTPA-enhanced MRI for the assessment of liver function and volume in liver cirrhosis. British J Radiol 86:20120653 doi: 20120610.20121259/bjr.20120653
12. Nishie A, Ushijima Y, Tajima T et al (2012) Quantitative analysis of liver function using superparamagnetic iron oxide-and Gd-EOB-

DTPA-enhanced MRI: Comparison with Technetium-99m galactosyl serum albumin scintigraphy. Eur J Radiol 81:1100–1104
13. Yamada A, Hara T, Li F et al (2011) Quantitative evaluation of liver function with use of gadoxetate disodium–enhanced MR imaging. Radiology 260:727–733
14. Van Beers BE, Pastor CM, Hussain HK (2012) Primovist, eovist: what to expect? J Hepatol 57:421–429
15. Tsuda N, Matsui O (2010) Cirrhotic rat liver: reference to transporter activity and morphologic changes in bile canaliculi—gadoxetic acid–enhanced mr imaging 1. Radiology 256:767–773
16. Bae KE, Kim SY, Lee SS et al (2012) Assessment of hepatic function with Gd-EOB-DTPA-enhanced hepatic MRI. Dig Dis 30:617–622
17. Katsube T, Okada M, Kumano S et al (2011) Estimation of liver function using T1 mapping on Gd-EOB-DTPA-enhanced magnetic resonance imaging. Invest Radiol 46:277–283
18. Messroghli DR, Greiser A, Fröhlich M, Dietz R, Schulz-Menger J (2007) Optimization and validation of a fully-integrated pulse sequence for modified look-locker inversion-recovery (MOLLI) T1 mapping of the heart. J Magn Reson Imaging 26:1081–1086
19. Nacif MS, Turkbey EB, Gai N et al (2011) Myocardial T1 mapping with MRI: comparison of look-locker and MOLLI sequences. J Magn Reson Imaging 34:1367–1373
20. Lee JJ, Liu S, Nacif MS et al (2011) Myocardial T1 and extracellular volume fraction mapping at 3 tesla. J Cardiovasc Magn Reson 13:75
21. Bosch J, Berzigotti A, Garcia-Pagan JC, Abraldes JG (2008) The management of portal hypertension: rational basis, available treatments and future options. J Hepatol 48:S68–S92
22. Cohen JA, Kaplan MM (1979) The SGOT/SGPT ratio—an indicator of alcoholic liver disease. Dig Dis Sci 24:835–838
23. Levitsky J, Mailliard ME (2004) Diagnosis and therapy of alcoholic liver disease. Semin Liver Dis 24:233–247
24. Yoon JH, Lee JM, Han JK, Choi BI (2014) Shear wave elastography for liver stiffness measurement in clinical sonographic examinations evaluation of intraobserver reproducibility, technical failure, and unreliable stiffness measurements. J Ultrasound Med 33:437–447
25. Kudo M, Zheng RQ, Kim SR et al (2008) Diagnostic accuracy of imaging for liver cirrhosis compared to histologically proven liver cirrhosis. Intervirology 51:17–26
26. Messroghli DR, Plein S, Higgins DM et al (2006) human myocardium: single-breath-hold mr t1 Mapping with High Spatial Resolution—Reproducibility Study1. Radiology 238:1004–1012
27. Kim KA, Park MS, Kim IS et al (2012) Quantitative evaluation of liver cirrhosis using T1 relaxation time with 3 tesla MRI before and after oxygen inhalation. J Magn Reson Imaging 36:405–410
28. Xl C, Tw C, Zl L et al (2013) Spleen size measured on enhanced mri for quantitatively staging liver fibrosis in minipigs. J Magn Reson Imaging 38:540–547
29. Barnhart HX, Barboriak DP (2009) Applications of the repeatability of quantitative imaging biomarkers: a review of statistical analysis of repeat data sets. Transl Oncol 2:231–235
30. Planchamp C, Montet X, Frossard J-L et al (2005) Magnetic resonance imaging with hepatospecific contrast agents in cirrhotic rat livers. Investig Radiol 40:187–194
31. Yoneyama T, Fukukura Y, Kamimura K et al (2013) Efficacy of liver parenchymal enhancement and liver volume to standard liver volume ratio on Gd-EOB-DTPA-enhanced MRI for estimation of liver function. Eur Radiol 24:857–865
32. Kötz B, West C, Saleem A, Jones T, Price P (2009) Blood flow and Vd (water): both biomarkers required for interpreting the effects of vascular targeting agents on tumor and normal tissue. Mol Cancer Ther 8:303–309
33. de Franchis R (2006) Noninvasive diagnosis of esophageal varices: is it feasible&quest. Am J Gastroenterol 101:2520–2522
34. Berzigotti A, Seijo S, Arena U et al (2013) Elastography, spleen size, and platelet count identify portal hypertension in patients with compensated cirrhosis. Gastroenterology 144:102–111
35. Motosugi U, Ichikawa T, Sou H et al (2009) Liver parenchymal enhancement of hepatocyte-phase images in Gd-EOB-DTPA-enhanced MR imaging: Which biological markers of the liver function affect the enhancement? J Magn Reson Imaging 30:1042–1046
36. Heye T, Yang S-R, Bock M et al (2012) MR relaxometry of the liver: significant elevation of T1 relaxation time in patients with liver cirrhosis. Eur Radiol 22:1224–1232
37. de Bazelaire CM, Duhamel GD, Rofsky NM, Alsop DC (2004) MR imaging relaxation times of abdominal and pelvic tissues measured in vivo at 3.0 T: preliminary results1. Radiology 230:652–659
38. Li W, Griswold M, Yu X (2010) Rapid T1 mapping of mouse myocardium with saturation recovery look-locker method. Magn Reson Med 64:1296–1303
39. Liberman G, Louzoun Y, Ben Bashat D (2014) T1 Mapping using variable flip angle SPGR data with flip angle correction. J Magn Reson Imaging 40:171–180
40. Nilsson H, Blomqvist L, Douglas L, Nordell A, Jonas E (2010) Assessment of liver function in primary biliary cirrhosis using Gd-EOB-DTPA-enhanced liver MRI. HPB 12:567–576
41. Leinhard OD, Dahlström N, Kihlberg J et al (2012) Quantifying differences in hepatic uptake of the liver specific contrast agents Gd-EOB-DTPA and Gd-BOPTA: a pilot study. Eur Radiol 22:642–653
42. Saito K, Ledsam J, Sourbron S et al (2013) Assessing liver function using dynamic Gd-EOB-DTPA-enhanced MRI with a standard 5-phase imaging protocol. J Magn Reson Imaging 37:1109–1114
43. Stockmann M, Lock JF, Malinowski M, Niehues SM, Seehofer D, Neuhaus P (2010) The LiMAx test: a new liver function test for predicting postoperative outcome in liver surgery. HPB 12:139–146
44. Fan S, Wang Q, Lo C, Yu K, Lai E, Wong J (1994) Evaluation of indocyanine green retention and aminopyrine breath tests in patients with malignant biliary obstruction. Aust N Z J Surg 64:759–762